RSC Chemical Biology

ROYAL SOCIETY OF CHEMISTRY

PAPER

View Article Online
View Journal | View Issue

Cite this: *RSC Chem. Biol.*, 2025, 6, 387

Siderophore-based targeted antibody recruitment for promoting immune responses towards Gram-negative pathogens†

Seungwoo Kim,[a] Ho-Sung Park,[b] Do Young Kim,[a] Hyunhi Joh,[a] Jiseok Oh,[a] Dong Ho Kim,[b] Min Ju Kang,[b] Chul Hee Choi*[b] and Hak Joong Kim*[a]

Received 1st December 2024,
Accepted 10th January 2025

DOI: 10.1039/d4cb00293h

rsc.li/rsc-chembio

Antibody-recruiting molecules (ARMs) have emerged as a promising strategy for enhancing immune responses against pathogens and cancer cells. In this study, we developed a novel class of antibacterial ARMs utilizing siderophores, small iron-chelating compounds, as targeting motifs. Siderophores naturally exhibit high specificity for bacterial pathogens due to their role in iron acquisition, making them ideal candidates for selective targeting. We identified a potent ARM, **GNP3**, comprising MECAM, a siderophore mimetic, and 2,4-dinitrophenyl (DNP), a motif recognized by endogenous antibodies, connected *via* a flexible linker. **GNP3** binds simultaneously to both anti-DNP antibody and the siderophore receptor, FepA, facilitating the targeted deposition of antibodies on the surface of FepA-expressing bacterial cells, such as *Escherichia coli* and *Pseudomonas aeruginosa*. This **GNP3**-induced opsonization promoted robust immune responses, including complement-dependent cytotoxicity (CDC) in the presence of serum and macrophage-mediated phagocytosis. Moreover, **GNP3** effectively triggered CDC activity against serum-resistant uropathogenic *E. coli*. The results suggest that siderophore-based ARMs, by harnessing the immune defense system, represent a promising complementary approach to traditional antibiotics for overcoming recalcitrant bacterial infections.

Introduction

The widespread antibiotic resistance poses a serious challenge to treating bacterial infections by severely limiting available therapeutic options.[1,2] Additionally, many pathogens found in clinical settings show high resistance to human serum.[3,4] The humoral immunity provided by serum is a crucial first-line defense mechanism against invading pathogens, primarily through complement-dependent cell killing and phagocytic clearance. Such immune responses often begin with the opsonization of bacterial cells, where their surface is labeled with antibodies. Although serum resistance develops in various ways, a common mechanism involves altering cell surface architecture, allowing pathogens to evade antibody surveillance.[4,5] As such, the immunotherapy addressing these immune evasive behaviors in pathogens could provide an effective alternative and/or complement to antibiotics.

Recently, several research groups have explored a new antibacterial immunotherapy approach based on the use of bifunctional molecules, called "antibody-recruiting molecules" (ARMs).[6,7] These chemical modalities are designated to direct endogenous antibodies present in serum to bacterial surfaces, thereby stimulating immune responses. Structurally, they are composed of a bacterial surface-targeting ligand and a hapten recognizable by endogenous antibodies. The dinitrophenyl (DNP) moiety is the most frequently employed hapten for this purpose, because 1–2% of endogenous antibodies in human body recognize this motif.[8,9] Since the pioneering work by Schultz in 1991,[10] this passive vaccination approach has been applied primarily to developing anti-cancer agents. Recently, promising results have also been demonstrated in antibacterial applications.[11–21]

The judicious selection of a surface epitope is the crucial first step in generating a successful ARM. The epitopes exploited for bacterial killing thus far include mannose receptor,[11] lectin,[17] fibril protein,[18] and cell wall components[12–16,19–21] such as peptidoglycan and mycomembrane. Effective epitopes for bacterial killing should have high expression levels on the target pathogen, significant exposure to the extracellular environment, and cognate ligands with strong affinity.[18] In this context, we reasoned that siderophore

[a] *Department of Chemistry and Center for Proteogenome Research Korea University Seoul, 02841, Republic of Korea. E-mail: hakkim@korea.ac.kr*
[b] *Department of Microbiology and Medical Science Chungnam National University School of Medicine Daejeon, 35015, Republic of Korea. E-mail: choich@cnu.ac.kr*

† Electronic supplementary information (ESI) available. See DOI: https://doi.org/10.1039/d4cb00293h

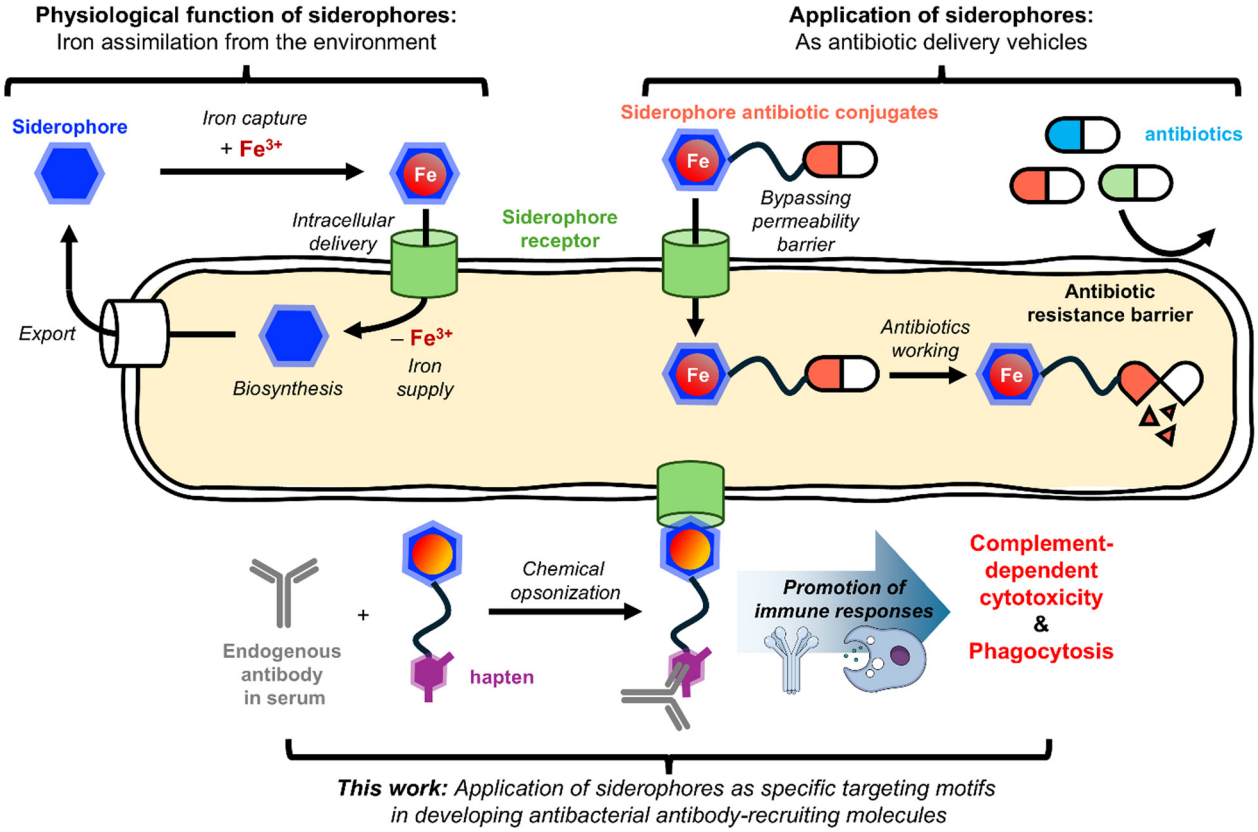

Fig. 1 Schematic overview of this work.

transporters would be suitable epitopes for developing antibacterial ARMs (Fig. 1).

Siderophores are natural chelators produced by most pathogens to assimilate iron, an essential nutrient, from the environment.[22–25] The intracellular iron supply *via* siderophores involves active transport through their cognate transporters. Siderophore transporters are displayed on membrane surfaces and, importantly, overexpressed in pathogens for their survival at infection sites. Additionally, siderophores bind tightly to their transporters,[26,27] thus making the siderophore-transporter pair an ideal target for ARM development.

Herein, we report that siderophore-DNP conjugates can direct anti-DNP antibodies to the surface of *Escherichia coli* and other Gram-negative pathogens, triggering their complement-dependent cytotoxicity (CDC) and phagocytosis. Moreover, this siderophore-based ARM was able to induce antibody-mediated cytotoxicity against serum-resistant uropathogenic *E. coli* (UPEC) strains, showcasing the potential of the ARM strategy exploiting siderophore receptors in overcoming serum resistance.

Results

The study to validate the siderophore-based ARM concept commenced with synthesis of a series of MECAM-DNP conjugates with systematically varied linker lengths. MECAM was selected as the targeting siderophore, because it is a well-established enterobactin (ENT) mimetic[28] and the uptake system for ENT is present in many Gram-negative pathogens. The synthesis process, inspired by a recent study on MECAM-antibiotic conjugates,[29] began with the nitration of 1,3,5-tris(bromomethyl)benzene (**1**) (Scheme 1). Subsequent substitution of the bromides in compound **2** with primary amines was achieved using ammonia. Next, the *O*-acetyl protected catechol moiety was then introduced to all amine groups using acyl chloride **3** (Scheme S1, ESI†), resulting in compound **4**. For effective incorporation of both the linker and DNP, a series of DNP-linked acyl chlorides (**5a–5d**) were prepared as delineated in Scheme S2 (ESI†). After reducing the nitro group of compound **4**, the resulting amine intermediate was treated with **5a–5d** in the presence of a base, followed by global deacetylation to yield the MECAM-DNP conjugates, **6a–6d**. Finally, to prevent any perturbation in the mobile iron level during biological characterization, these apo-compounds were complexed with Ga(III) ions to produce the corresponding holoforms, **GNP1–4** (**7a–7d**, respectively).

The first question to address was whether MECAM-DNP conjugates could recruit anti-DNP antibody to opsonize *E. coli*. For this purpose, *E. coli* BW25113 Δ*entA*, a mutant where ENT biosynthesis was impaired, was treated with **GNP1–4** in the presence of AF488-labeled anti-DNP antibody. The fluorescence microscopy analysis showed that all four conjugates were able to deposit the antibody on the surface of *E. coli*, in contrast to

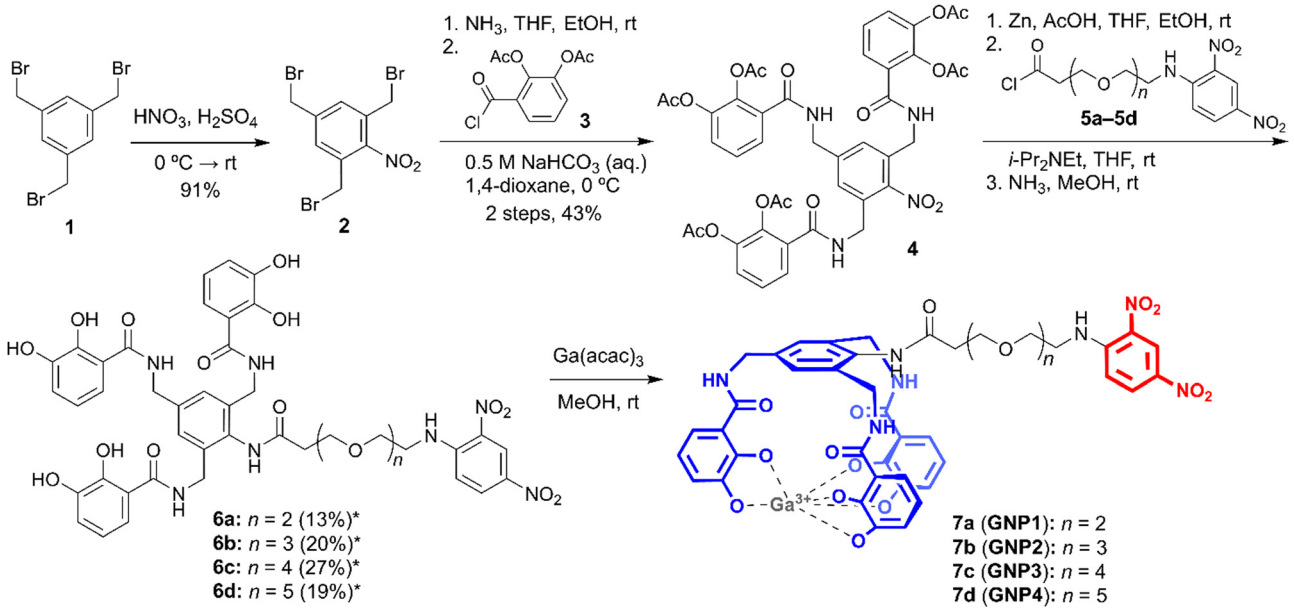

Scheme 1 Synthesis of Ga(III)-complexed MECAM-DNP conjugates, **GNP1–4** (MECAM in blue, DNP in red). * The presented yields indicate the results of the corresponding three-step processes.

Ga(III)-MECAM alone (Fig. 2A). Additionally, flow cytometry analysis showed that the linker length had significant influence on the antibody-recruiting efficiency, where **GNP3** was identified as the best ARM (Fig. 2B). Functional characterization of **GNP3** revealed that it exhibited neither cytotoxic effects on *E. coli* (Fig. S2 and S3, ESI†) nor promoted its growth under iron-deficient conditions (Fig. S4, ESI†).

Opsonization is a cell surface event and thus the antibody-recruiting activity of **GNP3** would depend on its interaction with a siderophore receptor located on the outer membrane (OM). To identify the specific OM receptor responsible for **GNP3**-induced opsonization, various *E. coli* mutant strains were treated with **GNP3**, along with AF488-labeled anti-DNP antibody, followed by fluorescence analysis. As illustrated in Fig. 2C and D, the labeling by **GNP3** vanished near completely in the absence of FepA, the primary OM receptor for ENT uptake, indicating that FepA is likely the target receptor for **GNP3**. By contrast, disruption of other components involved in siderophore uptake, such as alternative OM receptors (CirA and Fiu), a periplasmic binding protein (FepB), and an ATP-binding protein of the inner membrane permease complex (FepC), had marginal effects on the labeling efficiency of **GNP3**. Following the confirmation of successful MECAM-DNP conjugate-dependent antibody deposition, we investigated whether this promoted opsonization could translate into enhanced CDC. To evaluate this, *E. coli* strains were treated with human complement serum (HCS), the MECAM-DNP conjugate, and unlabeled anti-DNP antibody. Notably, we used HCS after lysozyme depletion to focus exclusively on complement pathway activation. As shown in Fig. 2E, **GNP3** exhibited the highest potency among the tested conjugates (**GNP1–4**), highlighting it as the most effective ARM.

The cytotoxicity induced by **GNP3** was dependent on the presence of both anti-DNP antibody and active HCS, because significant activity reduction was noted in the absence of either component (Fig. 2F). Intriguingly, substantial CDC activity was observed even without the exogenously added anti-DNP antibody, supporting the presence of DNP-recognizing antibodies in the endogenous antibody pool of HCS.[8,9] The failure to rescue activity by substituting anti-His antibody for anti-DNP antibody emphasized the necessity of specific antibody binding to the DNP motif. Furthermore, using heat-inactivated HCS did not induce bactericidal activity, reinforcing that **GNP3**-promoted cytotoxicity relies on active complement proteins. Moreover, **GNP3**-induced CDC appeared to require its concurrent binding to both anti-DNP antibody and FepA. This was evidenced by the observation of significant **GNP3** activity attenuation when competing molecules, Ga(III)-complexed MECAM/ENT and DNP ligand (**8c**, Scheme S2, ESI†), were introduced in 10-fold excess (Fig. 2G). Further analysis revealed that the CDC activity of **GNP3** was dependent on the presence of the FepA receptor (Fig. 2H), aligning with the opsonization test results. It is worth noting that disruption of *entA* enhanced the CDC activity of **GNP3**, likely due to the absence of competition between ENT and **GNP3** for FepA binding. Collectively, these findings successfully demonstrate that a well-designed siderophore-based ARM can effectively trigger CDC against a bacterium expressing the corresponding siderophore OM receptor by recruiting complement components to the bacterial surface *via* antibody-mediated mechanisms, as hypothesized.

Active uptake of ENT has been observed not only in *E. coli*, but also in other Gram-negative bacteria, suggesting that **GNP3** could potentially enhance the CDC against pathogens beyond *E. coli*. To explore this, the ability of **GNP3** to opsonize representative Gram-negative pathogens, *Acinetobacter baumannii*, *Klebsiella pneumoniae*, and *Pseudomonas aeruginosa*, was tested using fluorescence analysis. As shown in Fig. 3A and B,

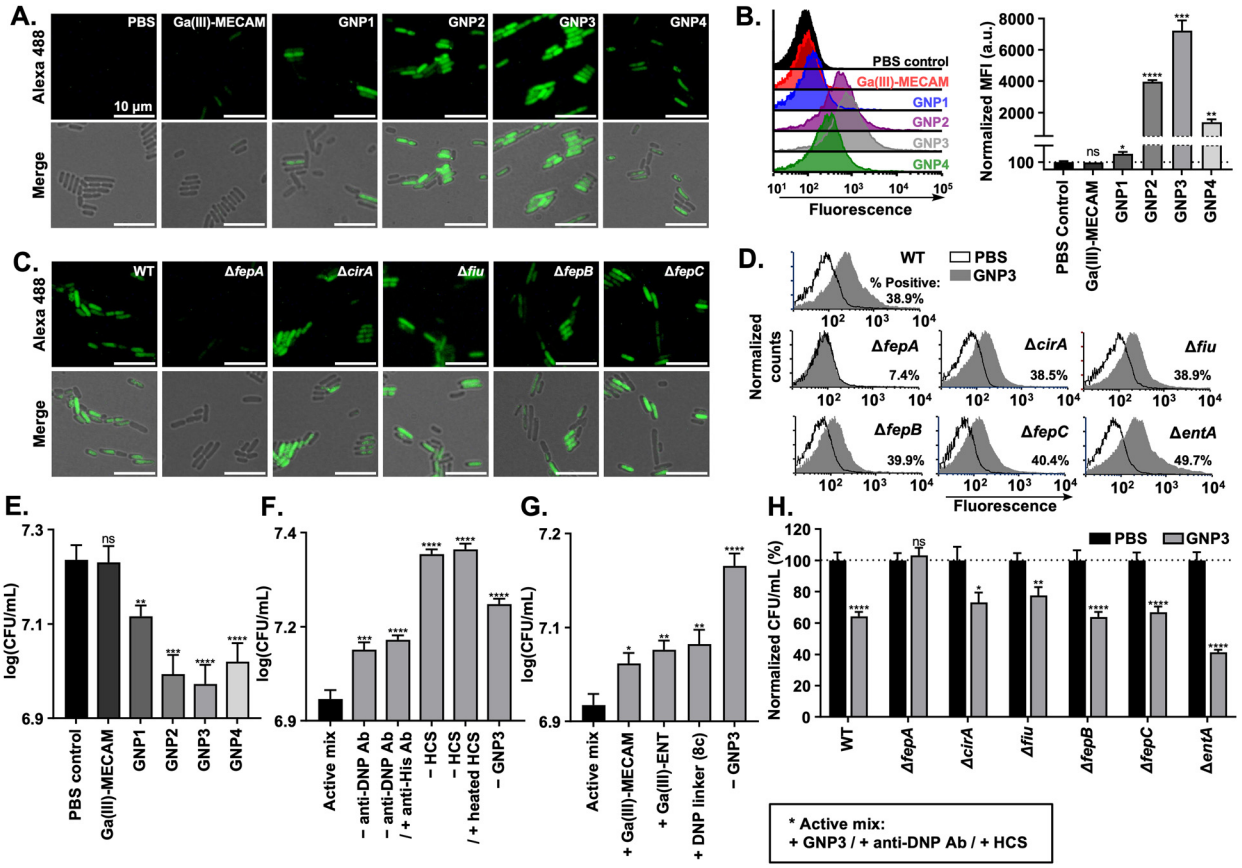

Fig. 2 Analysis of the opsonization and complement-dependent cytotoxicity (CDC) of *E. coli* induced by MECAM-DNP conjugates combined with anti-DNP antibody. Comparison of opsonization activity among **GNP1–4** using (A) fluorescence microscopy and (B) flow cytometry (n = 3). Identification of key components in the siderophore uptake machinery involved in **GNP3**-dependent opsonization using (C) fluorescence microscopy and (D) flow cytometry (n = 3). CDC assay results: (E) comparison of **GNP1–4** in CDC induction; (F) identification of essential elements for **GNP3**-dependent CDC; (G) confirmation of the need for simultaneous binding of **GNP3** to both the siderophore receptor and anti-DNP antibody for activity; and (H) differential responses of siderophore uptake mutants to **GNP3**-dependent CDC, confirming the importance of FepA in **GNP3** activity. In all assays, 100 nM **GNP1–4** (Fig. S1, ESI†), 0.02 mg mL^{-1} (*ca.* 130 nM) antibody, and 10% HCS (only for CDC assays) were used in pH 7.4 PBS buffer. Fluorescence images were acquired under consistent exposure settings and identically processed. Cytotoxicity was determined by colony forming unit (CFU per mL) measurements (n = 10) at 25 min time points after compound treatment (Fig. S5 and S6, ESI†). Data are presented as means ± standard error. Statistical significance was determined using two-tailed Student's t-tests (ns: not significant, *$p < 0.0332$, **$p < 0.0021$, ***$p < 0.0002$, ****$p < 0.0001$).

P. aeruginosa was the most efficiently opsonized organism by **GNP3** among these three bacteria, consistent with a recent report by Fritsch *et al.* that demonstrated efficient iron delivery by MECAM in *P. aeruginosa*.[30] Surprisingly, *A. baumannii* and *K. pneumoniae* were poorly labeled, despite both possessing close homologs to FepA, suggesting a likelihood of their interacting with MECAM.[31,32] Consistent with the opsonization results, *P. aeruginosa* was susceptible to **GNP3**-promoted CDC enhancement as shown in Fig. 3C, supporting the therapeutical potential of **GNP3** in controlling other Gram-negative pathogens.

Uropathogenic *E. coli* (UPEC) is the primary causative bacterium responsible for urinary tract infection and poses growing concerns due to its rising resistance to both antibiotics and humoral immunity.[33–35] A recent meta-analysis found that over 50% of UPEC strains exhibit genotypic traits linked to serum resistance.[36] To address this challenge, we explored a siderophore-based ARM strategy to determine whether it could increase the vulnerability of UPEC to CDC, thereby alleviating their serum resistance. We selected three UPEC strains for this investigation: CFT073, a well-established model strain, and two patient-derived strains, UPEC 26-1 and UPEC 39,[37] all of which demonstrated serum resistance. As illustrated in Fig. 3D and E, the fluorescence-based opsonization test revealed that **GNP3** could recruit anti-DNP antibodies to CFT073 and UPEC 26-1, but not to UPEC 39. Although the recruitment efficiency for CFT073 and UPEC 26-1 was lower than for *E. coli* BW25113, treatment with a combination of **GNP3**, HCS, and anti-DNP antibody resulted in significant bactericidal activity against these two strains (Fig. 3F). As predicted by the opsonization test results, no CDC activity was observed for UPEC 39. At this stage, the reason for the variation in opsonization efficiency across different strains is unclear. Intriguingly, all UPEC strains tested exhibited higher *fepA* expression levels compared *to E. coli* BW25113 (Fig. S10, ESI†), suggesting that the reprogrammed membrane structure, such as capsule formation and

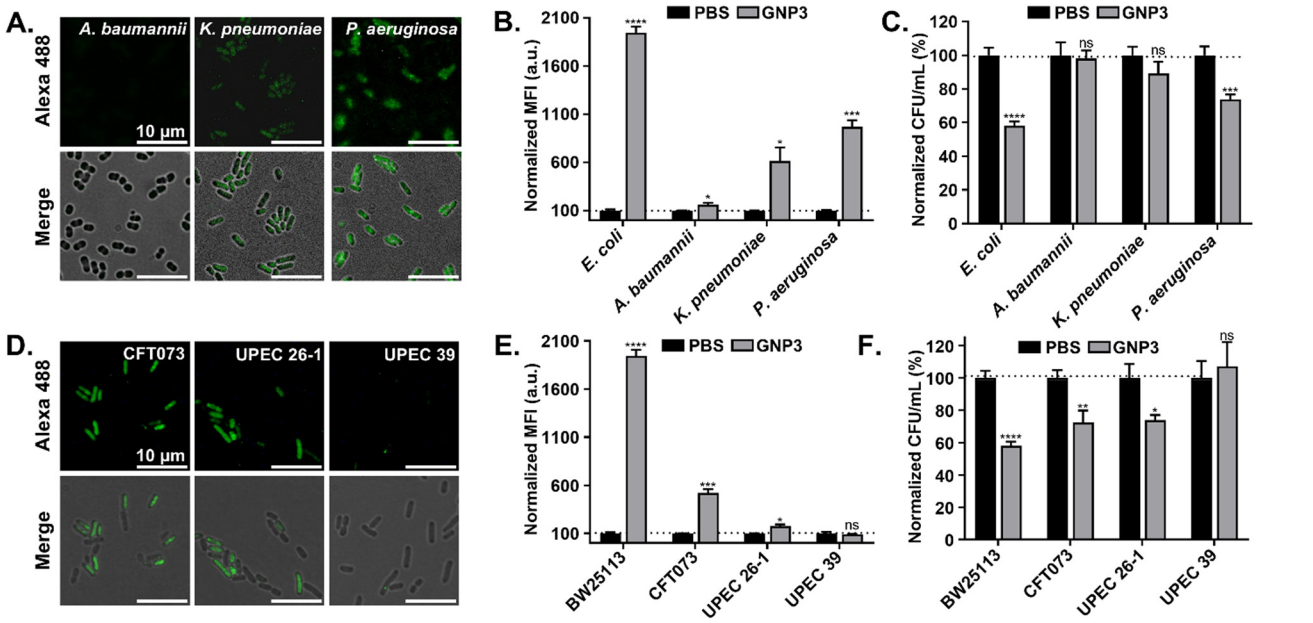

Fig. 3 Assessment of **GNP3** activity, in combination with anti-DNP antibody, against (A)–(C) various Gram-negative bacteria beyond *E. coli* and (D)–(F) serum-resistant uropathogenic *E. coli* strains. Opsonization activity assay results from (A) and (D) fluorescence microscopy and (B) and (E) flow cytometry (n = 3). (C) and (F) CDC activity assay results in the presence of HCS (n = 10) (Fig. S8 and S9, ESI†). In all assays, 100 nM **GNP3**, 0.02 mg mL^{-1} antibody, and 10% HCS (only for CDC assays) were used in pH 7.4 PBS buffer. Data are represented as means ± standard error. Statistical significance was determined by two-tailed Student's t-tests (ns: not significant, *$p < 0.0332$, **$p < 0.0021$, ***$p < 0.0002$, ****$p < 0.0001$).

modifications in the lipopolysaccharide layer, might be responsible for limiting the accessibility of anti-DNP antibodies and hence complement components. Nevertheless, the observed CDC induction by **GNP3** in CFT073 and UPEC 26-1 highlights that the antibody-recruiting strategy holds potential for counteracting serum resistance associated with UPECs.

Antibody deposition on the bacterial surface not only triggers CDC, but also enhances phagocytosis by immune cells such as macrophages and neutrophils. To investigate whether **GNP3**-promoted opsonization of *E. coli* could indeed enhance phagocytosis by macrophages, THP-1-derived macrophage cells were co-cultured with *E. coli* BW25113 cells, treated with either PBS or 100 nM **GNP3** in the presence of anti-DNP antibody. Following harvest of the co-cultured cells, the infected cells were stained with fluorescence dyes, AF568-conjugated phalloidin for actin and DAPI for nuclei visualization. As shown in Fig. 4A, confocal microscopic analysis revealed clearly enhanced phagocytosis in the sample IV treated with both **GNP3** and anti-DNP antibody, compared to the other controls (samples I–III). For more quantitative assessment, the intracellular bacterial cells engulfed by macrophages were counted by determining CFU per mL, which indicated that the enhancement of phagocytosis occurred owing to the presence of both **GNP3** and anti-DNP antibody (Fig. 4B). These observations align with the CDC assay results, supporting the conclusion that siderophore-based ARMs like **GNP3** can effectively promote bacterial clearance through enhancement of not only CDC, but also phagocytosis.

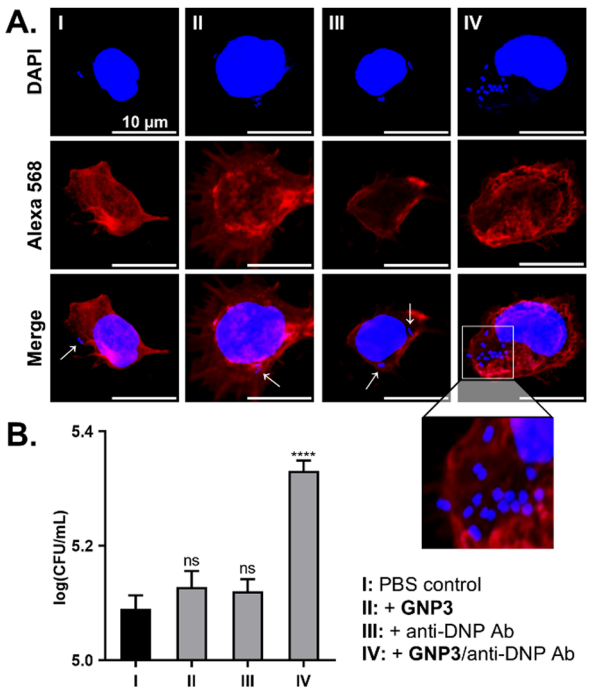

Fig. 4 Antibody-dependent phagocytosis assays. (A) Confocal microscopy images showing DAPI staining of nuclei in both macrophages and *E. coli* (blue), with AF568-conjugated phalloidin staining F-actin filaments (red). White arrows indicate engulfed *E. coli* cells. (B) Quantification of engulfed *E. coli* based on colony-forming unit (CFU) counts. Data are represented as means ± standard error (n = 10). Statistical significance was determined by two-tailed Student's t-tests (ns: not significant, ****$p < 0.0001$).

Conclusion

In this study, we demonstrated that siderophores can serve as effective bacteria-targeting motifs for developing ARMs. Specifically, the MECAM-DNP conjugate, **GNP3**, successfully opsonized bacterial cells expressing FepA in the presence of anti-DNP antibody, thereby promoting complement-mediated killing and phagocytosis. Using siderophores as targeting motifs offers several advantages. First, siderophore-based ARMs may be less prone to resistance development, as the siderophore uptake machinery is a key virulence factor essential for the survival of many pathogens at infection sites.[22–25] Second, the highly specific interactions between siderophores and their corresponding OM receptors suggest that siderophore-based ARMs would operate within a narrow spectrum, targeting only pathogens that express compatible OM receptors and thus minimizing perturbations in the human microbiota. This specificity is important from a safety perspective, because broad-spectrum ARMs carry a risk of excessive immune activation, which could be harmful to patients. Lastly, the small molecule nature of siderophores makes them more suitable for therapeutic development compared to previously reported antibacterial ARMs that use peptides, glycoconjugates, and aptamers as targeting motifs,[11,14,17,18,20] or require metabolic labeling to prime the bacterial surface.[12,13,15,19,21]

The utilization of siderophores in antibacterial development is not new. In particular, over the past few decades, they have been widely exploited as vehicles for the intracellular delivery of antibiotic drugs, with the primary goal of overcoming the membrane permeability barrier found in many antibiotic-resistant pathogens (Fig. 1).[38,39] These efforts have been fruitful, culminating in the recent clinical approval of the siderophore-based antibiotic, cefiderocol.[40] However, despite this progress, several challenges remain in developing effective siderophore-based antibiotic delivery systems. These include a limited molecular understanding of siderophore transport mechanisms and difficulties in delivering cytoplasmic antibiotics to target Gram-negative pathogens.[41] The current study has explored another new application of siderophores in ARM development. We specifically envisioned that the siderophore-based ARM modality could help alleviate serum resistance observed in serious pathogens. While the CDC assays using our most potent ARM, **GNP3**, against UPEC strains have shown encouraging results, the observed selective responses present the next challenge to address. This will require an in-depth examination of the serum resistance mechanisms and further structural optimization of the ARM. Nevertheless, given the rich repertoire of siderophores and their synthetic accessibility, we anticipate that next generation siderophore-based ARMs will overcome the current limitations of **GNP3** and be tailored to target a broader range of serious pathogens beyond *E. coli* and *P. aeruginosa* in near future.

Author contributions

S. W. Kim and H. J. Kim conceptualized the project. S. W. Kim, D. Y. Kim, H. H. Joh, and J. S. Oh performed synthesis and purification. S. W. Kim performed imaging of bacterial cells, flow cytometry, and CDC assay. H. S. Park, D. H. Kim, and M. J. Kang performed phagocytosis assay. H. J. Kim and C. H. Choi supervised the project and provided scientific guidance.

Data availability

All supplementary data, biological characterization procedures, and characterization data of all synthesized compounds are available in the ESI.†

Conflicts of interest

There are no conflicts to declare.

Acknowledgements

This work was supported by the Bio&Medical Technology Development Program and the Mid-career Research Grant of the National Research Foundation of Korea (NRF) funded by the Korean government (MSIT) (RS-2023-00259824 and NRF-2021R1A2C1094331, respectively) and the Korea Health Technology R&D Project Grant HR22C1734 through the Korea Health Industry Development Institute (KHIDI), funded by the Ministry of Health & Welfare.

Notes and references

1 A. R. Collaborators, C. J. Murray, K. S. Ikuta, F. Sharara, L. Swetschinski, G. R. Aguilar, A. Gray, C. Han, C. Bisignano, P. Rao, E. Wool, S. C. Johnson, A. J. Browne, M. G. Chipeta, F. Fell, S. Hackett, G. Haines-Woodhouse, B. H. K. Hamadani, E. A. P. Kumaran, B. McManigal, R. Agarwal, S. Akech, S. Albertson, J. Amuasi, J. Andrews, A. Aravkin, E. Ashley, F. Bailey, S. Baker, B. Basnyat, A. Bekker, R. Bender, A. Bethou, J. Bielicki, S. Boonkasidecha, J. Bukosia, C. Carvalheiro, C. Castañeda-Orjuela, V. Chansamouth, S. Chaurasia, S. Chiurchiù, F. Chowdhury, A. J. Cook, B. Cooper, T. R. Cressey, E. Criollo-Mora, M. Cunningham, S. Darboe, N. P. J. Day, M. D. Luca, K. Dokova, A. Dramowski, S. J. Dunachie, T. Eckmanns, D. Eibach, A. Emami, N. Feasey, N. Fisher-Pearson, K. Forrest, D. Garrett, P. Gastmeier, A. Z. Giref, R. C. Greer, V. Gupta, S. Haller, A. Haselbeck, S. I. Hay, M. Holm, S. Hopkins, K. C. Iregbu, J. Jacobs, D. Jarovsky, F. Javanmardi, M. Khorana, N. Kissoon, E. Kobeissi, T. Kostyanev, F. Krapp, R. Krumkamp, A. Kumar, H. H. Kyu, C. Lim, D. Limmathurotsakul, M. J. Loftus, M. Lunn, J. Ma, N. Mturi, T. Munera-Huertas, P. Musicha, M. M. Mussi-Pinhata, T. Nakamura, R. Nanavati, S. Nangia, P. Newton, C. Ngoun, A. Novotney, D. Nwakanma, C. W. Obiero, A. Olivas-Martinez, P. Olliaro, E. Ooko, E. Ortiz-Brizuela, A. Y. Peleg, C. Perrone, N. Plakkal, A. Ponce-de-Leon, M. Raad, T. Ramdin, A. Riddell, T. Roberts, J. V. Robotham, A. Roca, K. E. Rudd, N. Russell, J. Schnall, J. A. G. Scott, M. Shivamallappa, J. Sifuentes-Osornio, N. Steenkeste, A. J. Stewardson, T. Stoeva, N. Tasak, A. Thaiprakong, G. Thwaites, C. Turner, P. Turner, H. R. van Doorn, S. Velaphi, A. Vongpradith, H. Vu, T. Walsh,

S. Waner, T. Wangrangsimakul, T. Wozniak, P. Zheng, B. Sartorius, A. D. Lopez, A. Stergachis, C. Moore, C. Dolecek and M. Naghavi, *Lancet*, 2022, **399**, 629.
2 S. Walesch, J. Birkelbach, G. Jézéquel, F. P. J. Haeckl, J. D. Hegemann, T. Hesterkamp, A. K. H. Hirsch, P. Hammann and R. Müller, *EMBO Rep.*, 2023, **24**, e56033.
3 P. Lê-Bury, H. Echenique-Rivera, J. Pizarro-Cerdá and O. Dussurget, *FEMS Microbiol. Rev.*, 2024, **48**, fuae013.
4 H. Miajlovic and S. G. Smith, *FEMS Microbiol. Lett.*, 2014, **354**, 1.
5 J. D. Lambris, D. Ricklin and B. V. Geisbrecht, *Nat. Rev. Microbiol.*, 2008, **6**, 132.
6 P. J. McEnaney, C. G. Parker, A. X. Zhang and D. A. Spiegel, *ACS Chem. Biol.*, 2012, **7**, 1139.
7 W. Z. Charles, C. R. Faries, Y. T. Street, L. S. Flowers and B. R. McNaughton, *ChemBioChem*, 2022, **23**, e202200092.
8 F. S. Farah, *Immunology*, 1973, **25**, 217.
9 R. T. C. Sheridan, J. Hudon, J. A. Hank, P. M. Sondel and L. L. Kiessling, *ChemBioChem*, 2014, **15**, 1393.
10 K. M. Shokat and P. G. Schultz, *J. Am. Chem. Soc.*, 1991, **113**, 1861.
11 C. R. Bertozzi and M. D. Bednarski, *J. Am. Chem. Soc.*, 1992, **114**, 5543.
12 P. Kaewsapsak, O. Esonu and D. H. Dube, *ChemBioChem*, 2013, **14**, 721.
13 J. M. Fura, M. J. Sabulski and M. M. Pires, *ACS Chem. Biol.*, 2014, **9**, 1480.
14 S. A. Kristian, J. H. Hwang, B. Hall, E. Leire, J. Iacomini, R. Old, U. Galili, C. Roberts, K. B. Mullis, M. Westby and V. Nizet, *J. Mol. Med.*, 2015, **93**, 619.
15 M. J. Sabulski, S. E. Pidgeon and M. M. Pires, *Chem. Sci.*, 2017, **8**, 6804.
16 M. S. Feigman, S. Kim, S. E. Pidgeon, Y. Yu, G. M. Ongwae, D. S. Patel, S. Regen, W. Im and M. M. Pires, *Cell Chem. Biol.*, 2018, **25**, 1185.
17 J. Y. Hyun, C.-H. Lee, H. Lee, W.-D. Jang and I. Shin, *ACS Macro Lett.*, 2020, **9**, 1429.
18 M. N. Idso, A. S. Akhade, M. L. Arrieta-Ortiz, B. T. Lai, V. Srinivas, J. P. Hopkins, A. O. Gomes, N. Subramanian, N. Baliga and J. R. Heath, *Chem. Sci.*, 2020, **11**, 3054.
19 B. E. Dalesandro and M. M. Pires, *ACS Infect. Dis.*, 2021, **7**, 1116.
20 B. E. Dalesandro and M. M. Pires, *J. Med. Chem.*, 2023, **66**, 503.
21 P. Dzigba, A. K. Rylski, I. J. Angera, N. Banahene, H. W. Kavunja, M. C. Greenlee-Wacker and B. M. Swarts, *ACS Chem. Biol.*, 2023, **18**, 1548.
22 M. Miethke and M. A. Marahiel, *Microbiol. Mol. Biol. Rev.*, 2007, **71**, 413.
23 R. Golonka, B. S. Yeoh and M. Vijay-Kumar, *J. Innate Immun.*, 2019, **11**, 249.
24 J. Kramer, Ö. Özkaya and R. Kümmerli, *Nat. Rev. Microbiol.*, 2020, **18**, 152.
25 I. J. Schalk, *Nat. Rev. Microbiol.*, 2025, **23**, 24.
26 Z. Cao, Z. Qi, C. Sprencel, S. M. C. Newton and P. E. Klebba, *Mol. Microbiol.*, 2000, **37**, 1306.
27 R. C. Hider and X. Kong, *Nat. Prod. Rep.*, 2010, **27**, 637.
28 D. J. Ecker, B. F. Matzanke and K. N. Raymond, *J. Bacteriol.*, 1986, **167**, 666.
29 L. Pinkert, Y.-H. Lai, C. Peukert, S.-K. Hotop, B. Karge, L. M. Schulze, J. Grunenberg and M. Brönstrup, *J. Med. Chem.*, 2021, **64**, 15440.
30 S. Fritsch, V. Gasser, C. Peukert, L. Pinkert, L. Kuhn, Q. Perraud, V. Normant, M. Brönstrup and I. J. Schalk, *ACS Infect. Dis.*, 2022, **8**, 1134.
31 R. Koczura and A. Kaznowski, *Microb. Pathog.*, 2003, **35**, 197.
32 S. Subashchandrabose, S. Smith, V. DeOrnellas, S. Crepin, M. Kole, C. Zahdeh and H. L. T. Mobley, *mSphere*, 2015, **1**, e00013–e00015.
33 M.-D. Phan, K. M. Peters, S. Sarkar, S. W. Lukowski, L. P. Allsopp, D. G. Moriel, M. E. S. Achard, M. Totsika, V. M. Marshall, M. Upton, S. A. Beatson and M. A. Schembri, *PLoS Genet.*, 2013, **9**, e1003834.
34 M. Putrinš, K. Kogermann, E. Lukk, M. Lippus, V. Varik and T. Tenson, *Infect. Immun.*, 2015, **83**, 1056.
35 M. E. Terlizzi, G. Gribaudo and M. E. Maffei, *Front. Microbiol.*, 2017, **8**, 1566.
36 G. K. Bunduki, E. Heinz, V. S. Phiri, P. Noah, N. Feasey and J. Musaya, *BMC Infect. Dis.*, 2021, **21**, 753.
37 J. H. Lee, B. Subhadra, Y.-J. Son, D. H. Kim, H. S. Park, J. M. Kim, S. H. Koo, M. H. Oh, H.-J. Kim and C. H. Choi, *Lett. Appl. Microbiol.*, 2016, **62**, 84.
38 P. E. Klebba, S. M. C. Newton, D. A. Six, A. Kumar, T. Yang, B. L. Nairn, C. Munger and S. Chakravorty, *Chem. Rev.*, 2021, **121**, 5193.
39 B. Rayner, A. D. Verderosa, V. Ferro and M. A. T. Blaskovich, *RSC Med. Chem.*, 2023, **14**, 800.
40 T. Aoki, H. Yoshizawa, K. Yamawaki, K. Yokoo, J. Sato, S. Hisakawa, Y. Hasegawa, H. Kusano, M. Sano, H. Sugimoto, Y. Nishitani, T. Sato, M. Tsuji, R. Nakamura, T. Nishikawa and Y. Yamano, *Eur. J. Med. Chem.*, 2018, **155**, 847.
41 Y.-M. Lin, M. Ghosh, P. A. Miller, U. Möllmann and M. J. Miller, *Biometals*, 2019, **32**, 425.